Fe₃O₄ Nanoparticles as Additives for GAMMA-Ray Shielding: Structural and Surface Characterization

Violeta Nikolić[1]
Mirjana Milić[1]
Sonja Jovanović[1]
Vladimir Girman[2]

Monodisperse samples of magnetite nanoparticles in the size range of 5-13nm, were prepared by solvothermal synthesis and coprecipitation method. Obtained nanoparticles were characterized by different measurement techniques: X-ray diffraction analysis, transmission electron microscopy, selected area electron diffraction measurement, and Fourier transform infra-red spectroscopy. Measurements confirmed that the utilized synthesis methods are able to produce size and shape-controlled nanoparticles of a high-quality, that is of the technological importance. The results of the performed study represent the first stage in preparation of the Fe₃O₄ nanoparticles as an additive to concrete, which will be used for the construction of the special military facilities where it is necessary to provide a protection against γ-ray radiation.

Key words: **nanoparticles, nanomagnetite particles, morphological structure, additives, concrete, gamma ray radiation, radiation protection, facilities protection.**

Notations and symbols

ATR	– attenuated total reflection
d_{cr}	– crystallite diameter
FTIR	– Fourier transformation infra-red spectroscopy
hkl	– Miller indices of the plane
HRTEM	– high resolution transmission electron microscopy
JCPDS	– Joint Committee on Powder Diffraction Standards
SAED	– selected area electron diffraction
S1	– sample prepared by solvothermal method
S2	– sample prepared by coprecipitation method (nanoparticles obtained from ferrofluid)
S3	– sample prepared by coprecipitation method (nanoparticles obtained from precipitate)
TEM	– transmission electron microscopy
Δ	– wavenumber separation value
λ	– Cu Kα radiation wavelength
θ	– Bragg angle

Introduction

ONE of the most challenging problems during the last century was to face with electromagnetic interference pollution [1-3]. Electromagnetic pollution has been significantly increased during the 20th century, due to the technological progress of the humanity. Prominent problem, which has not yet been solved, is that the electromagnetic interference disturbs functioning of devices, equipment, and systems used for commercial, industrial and military applications [4, 5]. The type and the amount of shielding needed for electromagnetic radiation protection depends on the penetrability of the radiation [6]. It is important to point out that, compared to the other types of ionizing radiation, gamma radiation is characterized by the highest penetration power [7]. Protection against the gamma radiation should enable the reduction of the environmental electromagnetic background and suppress the appearance of secondary waves.

Due to the electrical neutrality of gamma rays, the interaction between gamma radiation and matter represents a statistical phenomenon. Efficiency of the gamma radiation shielding depends on the energy of the gamma ray, as well as on the nature of the absorbing material [6]. The absorbent material that could be used for the shielding of the gamma radiation is modified concrete [8, 9]. Conventional concrete represents a material whose properties are dependent on the constituents of the mixture. Since nanomaterials exhibit advanced properties compared to the bulk materials, nanoparticles are often used to improve the properties of the compact materials [10-14]. The effectiveness of concrete as a gamma radiation shield is significantly improved by the addition of the magnetic nanoparticles additives [15-17], since concrete belongs to the group of dielectrics [18]. Reinforced with Fe₃O₄ nanoparticles, concrete was found to be a suitable material for the suppression of gamma radiation [4]. Usage of Fe₃O₄ nanoparticles as an additive for γ-ray shielding requires the preparation of the size-limited Fe₃O₄ nanoparticles. Noteworthy, the above mentioned size depends on the energy of gamma radiation. For instance, literature data revealed that suitable size of the magnetite nanoparticles, used as additives for shielding of radiation with frequency 0.7 GHz, is~ 12 nm [4].

On the other hand, it is well known that the structural and morphological properties of the nano Fe₃O₄ determine its application. At the same time, the particles properties are significantly different depending on the chosen preparation method. Application of the nanoparticles as the additives for

[1] University of Belgrade, Vinča Institute of Nuclear Sciences, Mike Petrovića Alasa 12-14, P.O. Box 522, 11001 Belgrade, SERBIA
[2] Pavol Jozef Šafárik University, Institute of Physics, Department of Condensed Matter Physics, Park Angelinum 9, 04154 Košice, SLOVAKIA
  Correspondence to: Violeta Nikolić; e-mail: violeta@vin.bg.ac.rs

radiation shielding implies the preparation of the samples characterized by uniformity in the particles size and shape.

In this study, two different synthesis routes were employed to prepare an appropriate candidate, containing Fe$_3$O$_4$ nanoparticles additive, for the gamma radiation shielding: solvothermal synthesis and coprecipitation method. Expected size of the particles prepared by solvothermal synthesis is under 10 nm, and does not fulfill the size criteria necessary for the above mentioned application. For that reason, this synthesis method was performed in order to prepare nanoparticle seeds, whose size will be increased via seed-mediated solvothermal growth. On the other hand, coprecipitation method enables synthesis of the particles that fulfill size limitation required for the preparation of the additive for gamma radiation shielding. Comparative study of the structural and surface properties of the samples obtained in three different ways was performed, in order to determine compatibility of the prepared nanoparticles for use as the additives for protection against γ-ray irradiation of the special military facilities used by an army (underground command and telecommunication centers, special storage facilities of war material, water tanks, etc.).

X-ray diffraction (XRD) measurements were done by a Rigaku RINT-TTRIII using *CuKα* (λ = 1.5418 A). Diffraction patterns were recorded in the 2θ range: 10-70°, with a scanning rate 0.02 °/min. Qualx Program was used for data analysis. Fourier transformation infra-red (FTIR) spectroscopy was performed by Nicolet IS 50 FTIR Spectrometer, in the mid infra-red region. Sampling technique used to collect spectra was attenuated total reflectance (ATR). Data were analyzed by the Program Omnic. Transmission electron microscopy (TEM) was done by collecting micrographs at Jeol JEM 2100 transmission electron microscope operating at 200 kV. Images were processed in the Program ImageJ.

Experimental results and discussion
Synthesis of the samples
Solvothermal synthesis of the sample S1

Sample S1 was prepared by the solvothermal method. Fe(SO$_4$)·7H$_2$O was used as a precursor of the iron ions [19]. Solution of the sodium hydroxide, water, ethanol and oleic acid was prepared in molar proportion 1:2.2:0.8:0.2. Precursors were magnetically mixed for 30 minutes at the room temperature; afterwards, another solution, obtained by dissolving 0.56g of the Fe(SO$_4$)·7H$_2$O in 14 ml of H$_2$O was added in the stirring mixture, and stirred for 15 minutes. Then, the solution was shifted to teflon autoclave, where it was kept at 180°C for 10h. Cooled solution was washed with ethanol and n-hexane (in the volume proportion 1/3:2/3), at least three times. Washed precipitate consisted of Fe$_3$O$_4$/OA nanoparticles, and it was dried at 80°C for 2h.

Coprecipitation synthesis of the samples S2 and S3

Sample S2 was obtained by the coprecipitation method, using FeCl$_2$·4H$_2$O and FeCl$_3$·6H$_2$O salts as precursors of the iron ions [20]. 5.4g FeCl$_2$·4H$_2$O and 13.52g FeCl$_3$·6H$_2$O were separately dissolved in 10 ml H$_2$O, in the UV bath. After homogenization of the mixtures, solution of the Fe^{2+} ions had been added to the solution of the Fe^{3+} ions. In another beaker 20 ml H$_2$O was added. Under the magnetic stirring, the drop of the homogenized solution of the iron salts was added into the 20 ml H$_2$O. Then, a drop of the ammonia was put into the stirring solution, to start the nucleation process. Afterwards, the mixture of the iron salts was added into the stirring glass

at once. To the obtained solution, 17 ml ammonia was added dropwise. 150 ml H$_2$O was added to the prepared mixture, and the solution was stirred further for 30 minutes. The solution was placed onto the permanent magnet, to separate coprecipitate. Washing of the coprecipitate was performed with distilled water, at least three times. After the third washing, ph of the solution was 9.5. To decrease ph, 1M HCl was added until the solution ph reached the value 5.7, and then the solution was dialyzed against 0.001 M HCl solution. After the dialysis process had been finished (*ph*=3), the solution was again placed onto the permanent magnet, until the precipitate was separated. Certain amount of the prepared ferrofluid was dried at 60°C for 48h, and the obtained powder was labeled as sample S2, while the coprecipitate was dried under the equal conditions, and labeled as a sample S3.

In the Table 1. labels of the samples and synthesis methods used in this study are shortly presented.

Table 1. Samples labels and performed preparation method.

Sample	Preparation method
S1	Nanoparticles obtained by solvothermal synthesis
S2	Coprecipitation [nanoparticles from ferrofluid]
S3	Coprecipitation [nanoparticles from coprecipitate]

Structural analysis

Structural analysis of the samples was performed by the X-ray diffraction and TEM measurements.

a)

b)

c)

d)
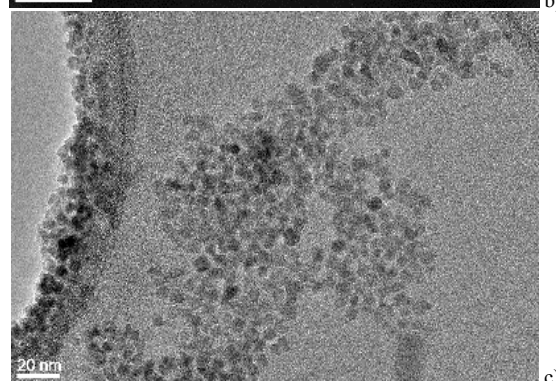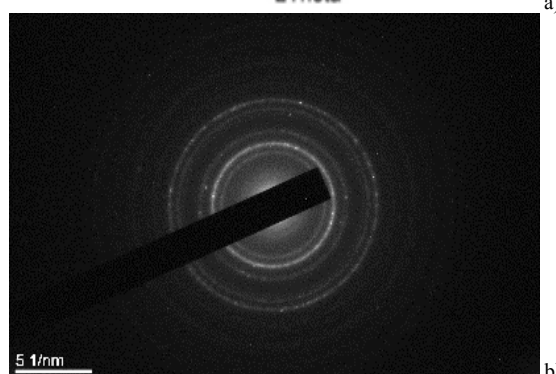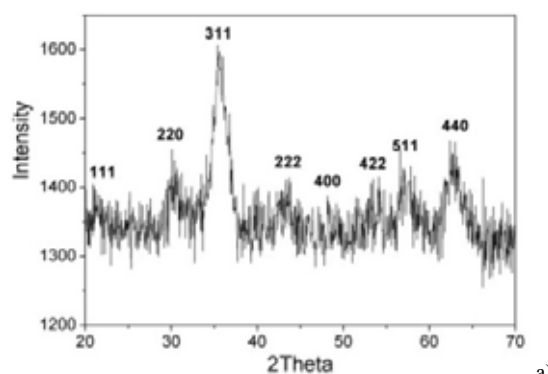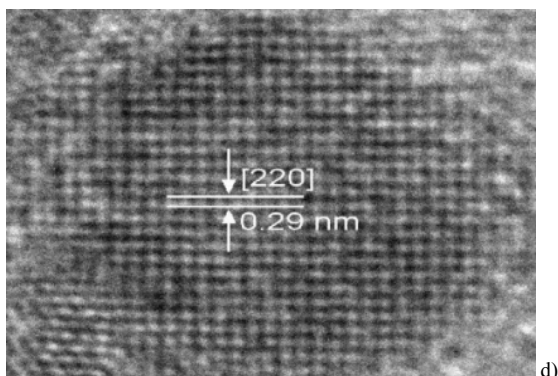
Figure 1. Images of the sample S1: a) XRD pattern; b) SAED pattern; c) TEM image; d) HRTEM.

Fig.1.a) presents diffraction pattern of the sample S1. Position of the diffraction maxima confirmed that the examined samples possess cubic spinel structure (JCPDS Qualx card: 00-900-2674, space group: Fd3m). From the position of the most pronounced diffraction maximum at $2\Theta=35°$, average crystallite size was determined by using the Scherrer's formula, and assuming that the nanoparticles are spherical in shape. Estimated crystallite size of the particles S1 was 5 nm. Since both magnetite and maghemite are characterized by the spinel structure (inverse and normal, respectively), X ray diffraction technique is not suitable to confirm the presence neither of the magnetite nor of the maghemite nanoparticles in the investigated sample.

Figures 1b)-d) show results of the TEM measurements. SAED measurement confirmed the formation of the magnetite phase, while the transmission electron micrographs were used to analyze the particles size and shape. According to the observed SAED diffraction rings (Fig.1b)), determined inter plane distances could be attributed to the Fe₃O₄ phase (Table 2).

Table 2. Estimated inter plane distances of the sample S1

Estimated inter plane distances [nm]	Theoretical values of the inter plane distances (JCPDS: 00-900-2674) [nm]	hkl indices of the corresponding plane
0.29283	0.29648	220
0.25452	0.25284	311
0.2111	0.20965	400
0.17476	0.14824	422
0.16162	0.16138	511
0.15005	0.14824	440

Diffraction rings in the SAED pattern are well pronounced and consistent with the X-ray diffraction pattern (Fig.1a)), demonstrating a high crystallinity of the particles. TEM micrographs of the sample S1 are shown in Fig.1c) and d). Images confirmed that particles are monodisperse and spherical in shape. The determined mean value of the particles size is 5nm (Fig.1c)), which is in a very good agreement with the crystallite size value extracted from the XRD measurement. The observed agreement points out to the single-crystal nature of the particles. HRTEM micrograph (Fig.1d)) enables observation of the lattice fringes, confirming high crystallinity of the sample. The determined interplane distance for 220 plane (0.29 nm) is in accordance with the SAED analysis.

Fig.2 shows the structural analysis of the sample S2. Cubic spinel structure of the sample S2 is observed at Fig.2a) (JCPDS Qualx card: 00-900-2674). The pronounced narrowing of diffraction maxima points to the bigger mean crystallite sizes (d_{cr}= 13 nm, according to $2\Theta=35°$) of the particles. Fig.2b) presents the SAED pattern of the sample S2, depicting to the magnetite presence (Table 3).

a)

b)

c)

d)
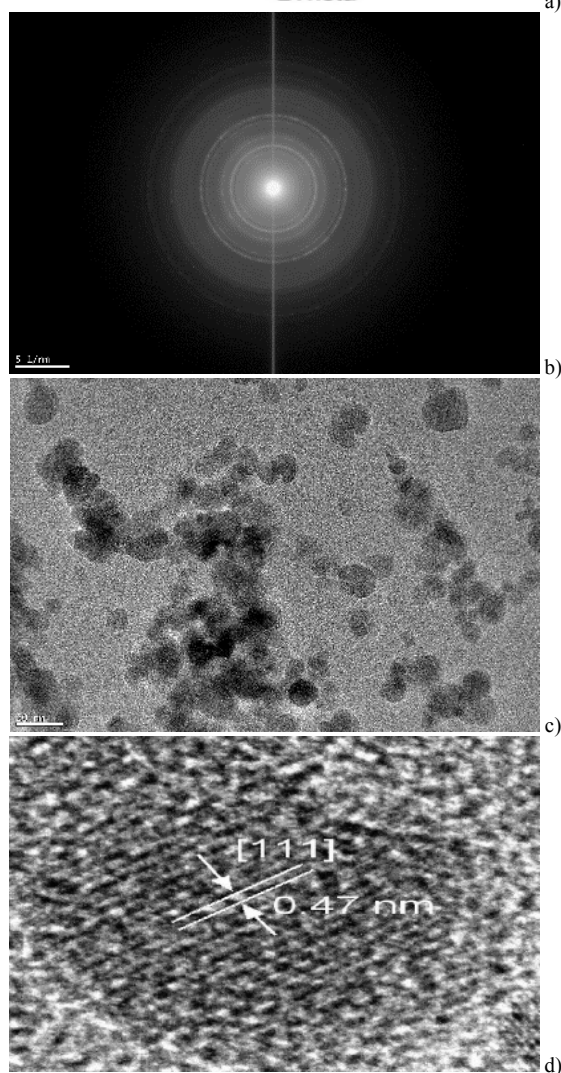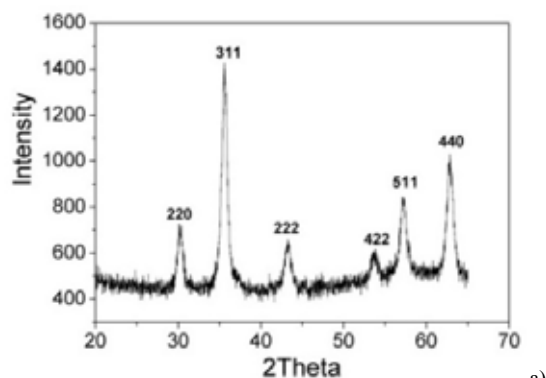
Figure 2. Images of the sample S2: a) XRD pattern; b) SAED pattern; c) TEM image; d) HRTEM image
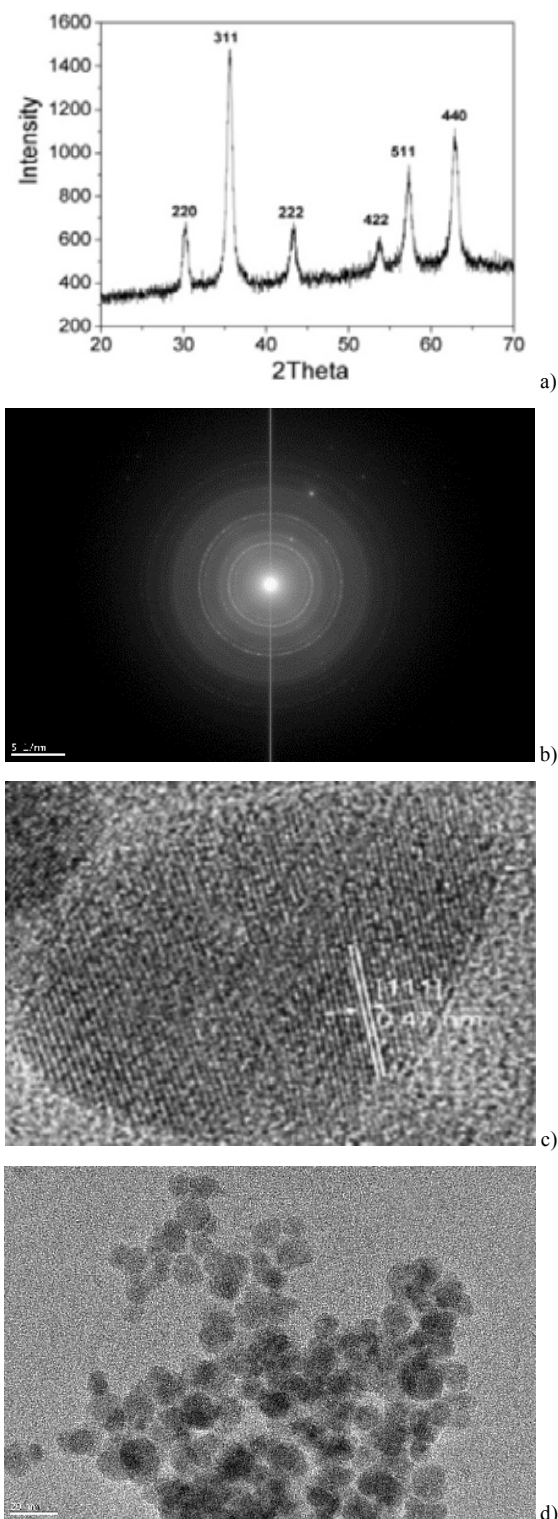
Table 3. Estimated interplane distances of the sample S2

Estimated inter-plane distances [nm]	Theoretical values of the inter plane distances (JCPDS: 00-900-2674) [nm]	hkl indices of the corresponding plane
0.29855	0.29648	220
0.25439	0.25284	311
0.21193	0.20965	400
0.15004	0.14824	440
0.16243	0.16138	511

Micrograph (Fig.2c)) shows rather uniform particle sizes (determined average size is 12 nm) of almost spherical nanoparticles. Fig.2d) presents HRTEM image, depicting to the nearly spherical shape of the nanoparticles. Clearly

observed lattice fringes pointed to the high crystallinity of the sample. Estimated interplane distance for 111 plane (0.47 nm) is in agreement with the theoretical value (0.48415 nm) and confirms the presence of the magnetite nanoparticles.

Fig.3 presents theresults of the structural investigation of the sample S3.

Figure 3. Images of the sample S3: a) XRD pattern; b) SAED pattern; c) TEM image; d) HRTEM

Sample 3 exhibited very similar diffraction pattern as the sample S2 (Fig.3a)). Mean crystallite size was estimated according to the position of the most pronounced diffraction maximum, d_{cr}= 13 nm. Fig.3b) shows SAED, that is confirming magnetite presence. Most pronounced interplane distances and corresponding planes are presented in Table 4.

Table 4. Estimated interplane distances of the sample S3

Estimated inter plane distances [nm]	Theoretical values of the inter plane distances (JCPDS: 00-900-2674) [nm]	hkl indices of the corresponding plane
0.26031	0.25284	311
0.21439	0.20965	400
0.17559	0.17117	422
0.15299	0.14824	440
0.16633	0.16138	511

TEM image (Fig.3c)) shows that the particles shape is nearly spherical: round and oval. Estimated mean particle size is 11 nm. HRTEM image enable more detailed observation of the particle shape; the particle is round, particularly more elongated (ellipticity is increased, compared to the samples S1 and S2). Sample S3 is also characterized by a high cristallinity, that is confirmed by the presence of the well-defined lattice fringes. The determined interplane distance, 0.47 nm, corresponds to the 111 plane of the magnetite, and represent an additional confirmation that the sample contains Fe₃O₄ nanoparticles.

TEM micrographs presented in Figures 2c) and 3c) displayed similar particles size, shape, as well as the similar degree of the particles agglomeration in the investigated samples. Nevertheless, the fact that the nanoparticles of the sample S3 precipitated at *ph*=3, while at the same time nanoparticles of the sample S2 remained in the solution forming a ferrofluid, points to the higher degree of agglomeration and wider particle size distribution of the sample S3. On the other hand, the preparation of the sample S2 for TEM measurements required drying of the ferrofluid, followed by dissolving of the obtained powder in the appropriate solvent. Since the coprecipitation synthesis did not involve the presence of the surfactant agent, as a result of these processes, the obtained sample expressed a higher degree of agglomeration compared to the ferrofluid nanoparticles, and more similar properties to the sample S3. It is important to point out that ferrofluid nanoparticles of the sample S2 are characterized by higher monodispersity and lower degree of agglomeration. The above properties of the S2 nanoparticles enable the formation of the ferrofluid, while the bigger, agglomerated nanoparticles, precipitate. On the contrary, due to the presence of the capping agent (oleic acid) the sample S1 retains a high monodispersity, regardless of the treatment performed to prepare the sample for the TEM measurement.

Structural analysis confirmed that all investigated samples are characterized by an inverse spinel structure, corresponding to the magnetite phase. According to the TEM results, a high crystallinity of the particles is observed. Particles possess mostly spherical morphology. Although all samples showed high monodispersity, the most pronounced monodispersity is observed for the sample S1, due to the presence of surfactant layer around each nanoparticle.

Surface analysis

FTIR spectroscopy was used to identify bonds attached to the particles surface, as well as to verify the presence of the magnetite or maghemite phase, since this technique is sensitive to the cation or vacancy order in the crystal. Figures 4a)-c) present FTIR spectra of the investigated samples.

Fig.4a) presents FTIR spectrum of the sample S1. Broad band centered around 3300 cm⁻¹ appeared as a result of the stretching of the hydroxide groups. Residue of the ethanol used during the washing procedure is observed through the appearance of the 1119 cm⁻¹ and 997 cm⁻¹ vibrations [21], attributed to the C-O stretching from ethanol and O-H out-of-plane bond, respectively. Further, observed broad bands in the

high-wavenumber region confirmed presence of the oleic acid capping of the magnetite nanoparticles. Bands at 2954 cm^{-1} and 2918 cm^{-1} originate from the symmetric CH_2 and asymmetric CH_2 vibrations of the oleic acid. Two broad bands, centered at 1523 and 1406 cm^{-1}, are linked to the asymmetric and symmetric C-O vibrations of the oleic acid [22, 23], pointing to the presence of the adsorbed oleic acid molecule onto the Fe_3O_4 active sites [24, 25]. Bidentate bridging value is determined based on the wavenumber separation value. Separation value in the wavenumber range: Δ=110-200 cm^{-1} is characteristic for bidentate bridging [24]. Estimated value, Δ=113 cm^{-1}, points to the chemisorbed oleic acid onto the Fe_3O_4 sites [24, 25]. In other words, COO^- group is covalently bonded to the Fe surface atoms.
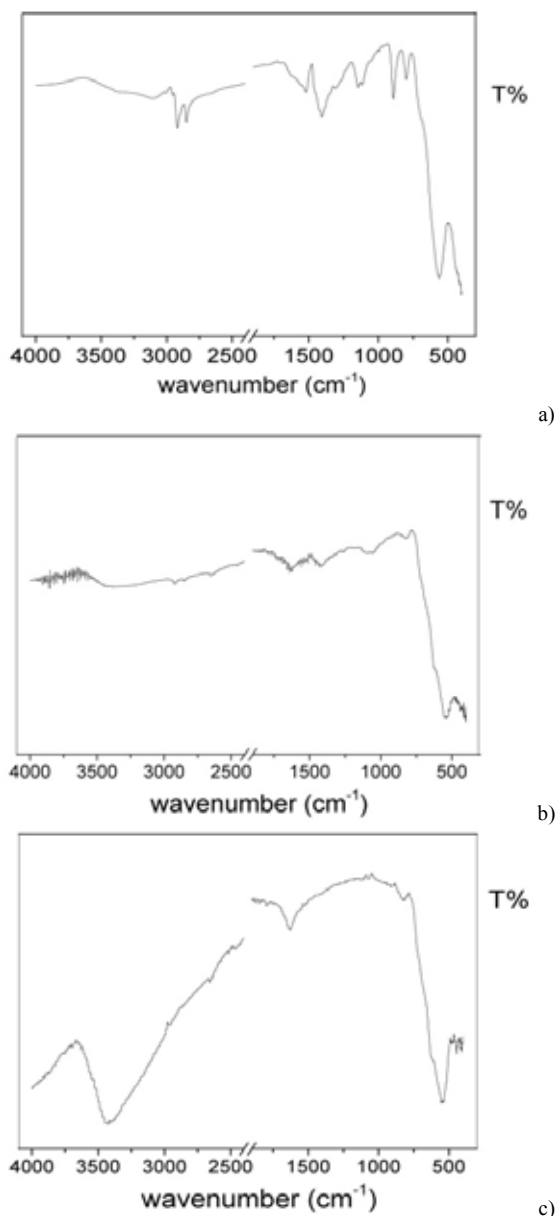

Figure 4. FTIR spectra of the investigated sample: a) S1; b) S2; c) S3

In the low-wavenumber region, which is a fingerprint area for the iron oxide vibrations, two bands observed at positions: 406 and 545 cm^{-1}, are attributed to the Fe-O vibrations, characteristic for stretching vibrations of metal ion at the tetrahedral A-site of the inverse spinel structure [26, 27]. The absence of the shoulder at 621 cm^{-1}, characteristic for maghemite [28], confirms the presence of the magnetite phase. According to the Fig.4a), the sample S1 contained Fe_3O_4 nanoparticles, which is in accordance with the Fig.1.

Fig.4a) also confirmed the presence of the capping agent-oleic acid. Oleic acid was used in the synthesis procedure to ensure the sample monodispersity, and to prevent oxidation of the particles and stoichiometry alteration that brings to the formation of the γ-Fe_2O_3 phase.

FTIR spectra of the samples S2 and S3 are presented at Figures 4b) and c), respectively. High wavenumber region displays the presence of intermolecularly bonded O–H groups in the samples (3300 cm^{-1} band). Also, the samples are characterized with the band at 1626 cm^{-1}, that is attributed to the H-O-H scissoring vibrations of free or adsorbed water. The band at 1455 cm^{-1} is ascribed to the O-H in-plane band, while the band at 997 cm^{-1} is assigned to the O-H out-of-plane vibration. Both samples show vibration at 550 cm^{-1}, that confirms the presence of the Fe ion at A-site of the spinel structure. On the other hand, in Fig.4c) the shoulder at 620 cm^{-1} is observed denoting the presence of the surface maghemite layer in the S3 sample, which is absent in the sample S2.

The observed presence of maghemite at the Fe_3O_4 surface is in accordance with the literature data, which defined magnetite as an oxide whose surface is always passivated by a maghemite layer, since magnetite oxidize immediately during the air exposure. Considering the fact that the samples S2 and S3 contained bare magnetite nanoparticles prepared without surfactant agent, stoichiometry of the magnetite nanoparticles obtained by coprecipitation is preserved by a static repulsion of the particles. The absence of the shoulder at 621 cm^{-1} in Fig.4a) and b) points to the fact that Fe_3O_4 nanoparticles of the samples S1 and S2 contain very thin surface layer of γ-Fe_2O_3, which is under the FTIR detectability threshold. According to the Fig.4c), sample S3 possesses ticker layer of the γ-Fe_2O_3 phase, placed on the Fe_3O_4 particles surface.

Conclusion

Three samples containing magnetite nanoparticles were prepared by two different chemical synthesis routes: solvothermal synthesis (S1) and coprecipitation method (S2 and S3). X-ray diffraction analysis confirms that the samples are characterized by the iron oxide spinel structure, without traces of the other iron oxide phase impurities. The samples prepared by different synthesis routes are characterized by different sizes, although all prepared samples displayed high-crystallinity. Mean particle size of the sample obtained by solvothermal synthesis was 5 nm, while the samples obtained by coprecipitation consisted of the particles bigger in size (d_{S2}=13 nm and d_{S3}=11 nm). TEM analysis shows that the particles of the investigated samples are mostly spherical in shape (round and oval). SAED analysis confirmed that the examined samples contained the magnetite nanoparticles. FTIR investigation revealed that the sample S1 possesses magnetite nanoparticles capped with oleic acid, while the samples S2 and S3 contained bare magnetite nanoparticles. Performed analysis of the samples shows that different synthesis methods resulted in the preparation of the high-quality nanoparticles. The studied samples could be further employed for the preparation of the concrete, reinforced with the synthesized particles, which will be utilized for the protection against gamma ray of the special military facilities used by an army.

Literature

[1] LING,J., ZHAI,W., FENG,W., SHEN,B., ZHANG,J.,ZHENG,W.G.: *Facile preparation of lightweight microcellular polyetherimide / graphene composite foams for electromagnetic interference shielding*, ACS applied materials & interfaces, 2013, Vol.5, No.7, pp.2677-2684.

[2] REDL,R.: *Electromagnetic environmental impact of power electronics equipment*, Proceedings of the IEEE, 2001, Vol.89, No.6, pp.926-938.

[3] CHEN,Y., WANG,Y., ZHANG,H.B., LI,X., GUI,C.X., YU.Z.Z.: *Enhanced electromagnetic interference shielding efficiency of polystyrene / graphene composites with magnetic Fe₃O₄ nanoparticles*, Carbon, 2015, Vol.82, No.3, pp.67-76.

[4] LESBAYEV,A.B., ELOUADI,B., BORBOTKO,T.V., MANAKOV, S.M., SMAGULOVA,G.T., BOIPRAV,O., PRIKHODKO,N.G.: *Influence of Magnetite Nanoparticles on Mechanical and Shielding Properties of Concrete, Eurasian Chemico-Technological Journal*, 2017, Vol.19, No.3, pp.223-229.

[5] MA,M.T., KANDA,M., CRAWFORD,M.L., LARSEN,E.B.: *A review of electromagnetic compatibility/interference measurement methodologies*, Proceedings of the IEEE, 1985, Vol.73, No.3, pp.388-411.

[6] https://sciencedemonstrations.fas.harvard.edu/presentations/α-β-γ-penetration-and-shielding, downloaded 12.12.2017.

[7] MORRISON,P.: *On gamma-ray astronomy*, Il Nuovo Cimento (1955-1965), 1958, Vol.7, No.6, pp.858-865.

[8] KHARITA,M.H., TAKEYEDDIN,M., ALNASSAR,M., YOUSEF,S.: *Development of special radiation shielding concretes using natural local materials and evaluation of their shielding characteristics*, Progress in Nuclear energy, 2008, Vol.50, No.1, pp.33-36.

[9] AKKURT,I., AKYLDIRIM,H., MAVI,B., KILINCARSLAN,S., BASYGIT,C.: *Gamma-ray shielding properties of concrete including barite at different energies*, Progress in Nuclear Energy, 2010, Vol.52, No.7, pp.620-623.

[10] NIKOLIĆ,V., TADIĆ,M., SPASOJEVIĆ,V.: *Thermal stability and magnetic properties of ε-Fe₂O₃ polymorph, 7th International Scientific Conference on Defensive Technologies*, OTEH 2016, 06-07. October, Military Technical Institute, Belgrade, SERBIA, ISBN 978-86-81123-82-9, 2016, pp.507-512

[11] NIKOLIĆ,V., TADIĆ,M., PANJAN,M., KOPANJA,L., CVJETIČANIN,N., SPASOJEVIĆ,V.: *Influence of annealing treatment on magnetic properties of Fe₂O₃/SiO₂ and formation of ε-Fe₂O₃ phase*, Ceramics International, 2017, Vol.43, No.3, pp.3147-3155.

[12] FABIAN,M., BOTTKE,P., GIRMAN,V., DUVEL,A., DA SILVA,K.L., WILKENING,M., HAHN,H., HEITJANS,P., SEPELAK,V.: *A simple and straightforward mechanochemical synthesis of the far-from-equilibrium zinc aluminate, ZnAl₂O₄, and its response to thermal treatment*, RSC Advances, 2015, Vol.5, No.2, pp.54321, DOI: 10.1039/c5ra09098a.

[13] MILIĆ,M., MATIĆ,M.V., LAZAROV,N.DJ.: *The dependence of critical temperature on oxygen concentration in YBa₂Cu₃O₆₊ₓ in terms of the fragmented chain model*, Central European Journal of Physics, 2011, Vol.9, No.3, pp.690-697.

[14] RICCI,A., POCCIA,N., CAMPI,G., CONERI,F., BARBA,L., ARRIGHETTI,G., POLENTARUTTI,M., BURGHAMMER,M., SPRUNG,M., ZIMMERMANN,M., BIANCONI,A.: *Networks of superconducting nano-puddles in 1/8 doped YBa₂Cu₃O₆.₅₊ᵧ controlled by thermal manipulation*, New Journal of Physics, 2014,Vol.16, No.5, pp.1-5,053030, DOI: 10.1088/1367-2630/16/5/053030.

[15] GENCEL,O., BROSTOW,W., OZEL,C., FILIZ M.: *Concretes containing hematite for use as shielding barriers*, Journal of Materials Science, 2010, Vol.16, No.3, pp.249-256.

[16] HORSZCZARUK,E., BRZOZOWSKI,P., SIKORA,P., CENDROWSKI,K., MIJOWSKA,E.: *The Effect of Nanomagnetite on the Shielding Properties of Cementitious Composites*, Construction Materials and Systems, 2017, Vol.55, No.5,pp.1-5.

[17] SHARIF,F., ARJMAND,M., MOUD,A.A., SUNDARARAJ,U., ROBERTS,E.P.: *Segregated Hybrid Poly (Methyl Methacrylate) / Graphene / Magnetite Nanocomposites for Electromagnetic Interference Shielding*, ACS Applied Materials & Interfaces, 2017, Vol.9. No.16, pp.14171-14179.

[18] SOUTSOS,M.N., BUNGEY,J.H., MILLARD,S.G., SHAW,M.R., PATTERSON,A.: *Dielectric properties of concrete and their influence on radar testing*, NDT & e International, 2001, Vol.34, No.6, pp.419-425.

[19] LI,C., WEI,R., XU,Y., SUN,A., WEI,L.: *Synthesis of hexagonal and triangular Fe₃O₄nanosheets via seed-mediated solvothermal growth*, Nano Research, 2014, Vol.7, No.4, pp.536-543.

[20] ILLES,E., TOMBACZ,E.: *The effect of humic acid adsorption on pH-dependent surface charging and aggregation of magnetite nanoparticles*, Journal of Colloid and Interface Science, 2006, Vol.295, No.1, pp.115–123.

[21] BRONSTEIN,L.M., HUANG,X., RETRUM,J., SCHMUCKER,A., PINK,M., STEIN,B.D., DRAGNEA,B.: *Influence of iron oleate complex structure on iron oxide nanoparticle formation*, Chemistry of Materials, 2007, Vol.19, No.2, pp.3624–3632, doi:10.1021/cm062948j.

[22] SOLER,M.A.G., ALCANTARA,G.B., SOARES,F.Q., VIALI,W.R., SARTORATTO,P.P.C., FERNANDEZ,J.R.L., SILVA,S.W., GARG,V.K., OLIVEIRA,A.C., MORAIS,P.C.: *Study of molecular surface coating on the stability of maghemite nanoparticles*, Surface Science, 2007, Vol.601, No.3, pp.3921-3925, DOI:10.1016 / j.susc.2007.04.029.

[23] LIN-VIEN,D., COLTHUP,N.B., FATELEY,W.G., GRASSELLI,J.G.: *The handbook of infrared and raman characteristic frequencies of organic molecules*, San Diego: Academic Press, 1991.

[24] LIMAYE,M.V., SINGH,S.B., DATE,S.K., KOTHARI,D., REDDY,V.R., GUPTA,A., SATHE,V., CHOUDHARY,R.J., KULKARNI,S.K.: *High coercivity of oleic acid capped CoFe₂O₄ nanoparticles at room temperature*, The Journal of Physical Chemistry B, 2009, Vol.113, No.27, pp.9070-9076.

[25] WU,N., FU,L., SU,M., ASLAM,M., WONG,K.C., DRAVID,V.P.: *Interaction of fatty acid monolayers with cobalt nanoparticles*, Nano letters, 2004, Vol.4, No.2, pp.383-386.

[26] CORNELL,R.M., SCWERTMANN,U.: *The iron oxides—structure, properties, reactions*, Occurences and Uses, Weinheim: Wiley-VCH, 2003.

[27] ISHII,M., NAKAHIRA,M., YAMANAKA,T.: *Infrared absorption spectra and cation distributions in (Mn,Fe)₃O₄*, Solid State Communications, 1972, Vol.11, No.2, pp.209–212.

[28] CHAMRITSKI,I., BURNS,G.: *Infrared - and Raman - Active Phonons of Magnetite, Maghemite, and Hematite: A Computer Simulation and Spectroscopic Study*, The Journal of Physical Chemistry B, 2005, Vol.109, No.11, pp.4965-4968.

Fe₃O₄ nanočestice kao aditivi za zaštitu od gama-zračenja: Strukturna i površinska karakterizacija

Monodisperzni uzorci nanočestica magnetita, veličine između 5-13 nm, su pripremljeni primenom solvotermalne sinteze i metode koprecipitacije. Karakterizacija sintetisanih nanočestica je izvršena primenom nekoliko mernih tehnika: difrakcija H-zraka, transmisiona elektronska mikroskopija, elektronska difrakcija sa odabrane površine i infra-crvena spektroskopija sa Furijeovom transformacijom. Merenja su potvrdila da se primenom pomenutih metoda sinteze dobijaju nanočestice visokog kvaliteta, što je od velikog tehnološkog značaja. Rezultati ove studije predstavljaju prvu fazu pripreme Fe₃O₄ nanočestica kao aditiva cementu pri njegovom korišćenju za izradu objekata specijalne namene gde je neophodno ostvariti zaštitu od γ-zraka.

Ključne reči: nanočestice, nanomagnetne čestice, morfološka struktura, aditivi, cement, gama zračenje, zaštita od zračenja, zaštita objekata.

Fe₃O₄ наночастицы как добавки для гама-радиационной защиты: Структурная и поверхностная характеризация

Монодисперсные образцы наночастиц магнетита, синтезированные в диапазоне размеров 5-13 нм, были получены методом сольвотермического синтеза и соосаждения. Характеристика синтезированных наночастиц осуществляется с использованием нескольких методов измерения: дифракции рентгеновских лучей, просвечивающей электронной микроскопии, дифракции электронов с выбранных областей и инфракрасной спектроскопии с преобразованием Фурье. Измерения подтвердили, что выполненные методы синтеза способны производить наночастицы с контролируемым размером и формой высокого качества, что имеет большое технологическое значение. Результаты проведённого исследования представляют собой первый этап подготовки наночастиц Fe3O4 в качестве добавок к цементу, который будет использован для строительства военных объектов специального назначения, где это необходимо для защиты от γ-излучения.

Ключевые слова: **наночастицы, наномагнитные частицы, морфологическая структура, добавки, цемент, гамма-излучение, радиационная защита, защита объектов.**

Nano particules Fe₃O₄ comme additifs pour la protection contre le rayonnement gamma: Caractérisation structurale et de surface

Les échantillons mono dispersés de nano particules de magnétite de taille de 5-13mm ont été préparés par l'application de la synthèse solvothermale et par la méthode de coprécipitation. La caractérisation des nano particules synthétisés a été obtenue par l'emploi de plusieurs techniques de mesure : diffraction des rayons X, microscopie électronique à transmission, diffraction électronique à partir d'une surface sélectionnée et la spectroscopie infrarouge à transformée de Fourier. Les mesurages ont confirmé que par l'utilisation des méthodes citées de synthèse on obtenait les nano particules de haute qualité ce qui est très important de point de vue technologique. Les résultats de cette étude représentent la première phase de la préparation des nano particules Fe3O4 comme un additif au béton pendant son emploi pour la construction des installations militaires spéciales où il est indispensable pour la réalisation de protection contre les rayons Y.

Mots clés: **nano particules, nano particules magnétiques, structure morphologique, additifs, béton, rayonnement gamma, protection contre le rayonnement, protection des installations.**